

## Structure and bonding of Group 13 monocarbonyls\*

Adam J. Bridgeman

University Chemical Laboratories, Lensfield Road, Cambridge CB2 1EW, UK

The geometries and vibrational frequencies of the lowest-lying spin-doublet and spin-quartet states of the monocarbonyl and isocarbonyl complexes of the elements of Group 13 have been studied using local density-functional calculations within the linear combination of Gaussian-type orbitals framework. An analogy is drawn between the familiar  $\sigma$  donation/ $\pi$ -back donation mechanism used to describe the bonding in transition-metal carbonyls and the bonding in these main-group molecules. Changes in orbital populations and bond orders upon complexation have been used to quantify this idea. The results strongly suggest that the species detected by the observation of characteristic metal–carbonyl stretching frequencies in matrices containing boron, aluminium and gallium together with carbon monoxide are the carbonyl complexes rather than the isocarbonyl isomers. The ground state of BCO is predicted to be a  $^4\Sigma^+$  state but the ground states of the remaining monocarbonyls are likely to be spin doublets. The  $^2\Pi$  state of BCO and AlCO may be unstable to bending probably because of the repulsive interaction between the metal  $s^2$  electrons and the donor electron pair on the ligand. This repulsion is much reduced in the  $^4\Sigma^+$  state and together with increased  $\pi$ -back donation this results in considerably stronger M–CO bonds. The  $\sigma$ -acid and  $\pi$ -base behaviour of the metals parallels their electronegativity.

Carbonyl complexes are known of almost all transition metals. The description<sup>1,2</sup> of the metal–carbon monoxide bond as involving  $\sigma$  donation from the ligand and  $\pi$ -back donation from metal d orbitals is an important paradigm in modern inorganic, organometallic and surface chemistry. For many years it was assumed that only transition metals were able to form simple carbonyls. Condensation of main-group metal atoms with carbon monoxide in inert matrices however results in the formation of products with characteristic C=O stretch peaks in their infrared spectra. For the elements of Group 13, monocarbonyls have been detected spectroscopically for boron,<sup>3,4</sup> aluminium<sup>5–7</sup> and gallium.<sup>7</sup> The present study is concerned with the bonding and structure of these complexes. These systems comprise a convenient set for an investigation of the bonding of CO to metals without accessible d electrons and for comparisons with the more thoroughly investigated transition-metal analogues. These are also simple models for the co-ordination of CO to main-group metal surfaces. The results of calculations using the linear combination of Gaussian-type orbitals–density functional (LCGTO-DF) method on the MCO and MOC molecules with M = B, Al, Ga or In are reported. A description and comparison of the bonding in these molecules is most easily obtained by one level of theory and equivalent basis sets.

The bonding between metal atoms and carbon monoxide is of considerable interest to both the molecular and surface chemist and has been studied extensively using a variety of theoretical methods. The strength of the metal–carbon bond in monocarbonyls is found to be very sensitive to the atomic configuration of the metal because of the repulsive interaction between metal  $\sigma$  electrons and the  $5\sigma$  lone pair of CO. Bagus *et al.*<sup>8</sup> studied the bonding between CO and atoms of sodium, magnesium and aluminium with a variety of electronic configurations. The Al–CO interaction, for example, was found to be strongly repulsive if the metal was taken to have a  $(3s_\sigma)^2(3p_\sigma)^1$  configuration. With a metal  $(3s_\sigma)^2(3p_\pi)^1$  configuration however the interaction with CO is only slightly repulsive. Promotion of sodium and magnesium atoms to the excited  $(3p_\pi)^1$  and  $(3p_\sigma)^1(3p_\pi)^1$  configurations respectively similarly led to more bonding interactions with CO. The repulsive role of metal  $\sigma$  electrons is also a feature of the bonding of transition-metal monocarbonyls. A study of NiCO by Rives and Fenske<sup>9</sup>

predicted a  $^1\Sigma^+$  ground state in contrast to previous work which predicted a spin-triplet ground state. The bonding in this molecule has been extensively studied.<sup>9–14</sup> The ground state results from the nickel atom with the excited  $3d^94s^1$  configuration. This configuration allows sd hybridization to occur with spin pairing in an sd hybrid perpendicular to the M–CO bond. This results in a decrease in the repulsive interaction of the  $5\sigma$  lone pair of CO with the metal s electron and a subsequent increase in the  $\pi$ -back donation. The increased bonding to CO is found to compensate the promotion energy required to promote the metal into the spin-paired excited configuration.

The tendency of transition metals to adopt excited  $3d^{n-1}4s^1$  configurations to reduce the  $\sigma$  repulsion is found<sup>15–19</sup> in other transition-metal monocarbonyls. As for NiCO, the repulsive  $4s$ – $5\sigma$  may be reduced still further by spin pairing either two d electrons or one s and one d at the cost of losing exchange energy. The molecules MnCO, FeCO, CoCO and NiCO are predicted<sup>17,18</sup> to have *low-spin* ground states. The low-spin states of the remaining monocarbonyls are predicted to be excited states but to be more strongly bonded than the ground states. The interaction of CO with a metal surface may be modelled by studies of its bonding to small clusters of metal atoms. Such studies<sup>20</sup> mirror the monocarbonyl calculations in predicting high spin–low spin crossovers to increase the bonding of the CO molecule resulting in local reduction in the paramagnetism of the cluster.

Fournier has recently published<sup>17,18</sup> studies on the monocarbonyls of the first-row transition metals. These highlighted the trends in  $\sigma$  donation and  $\pi$ -back bonding from carbonyl to metal along this series. In particular, the repulsive role of the metal 4s electrons was demonstrated.

The bonding between a main-group metal and carbon monoxide can be described in an analogous manner to that conventionally used for transition-metal carbonyls. The highest-occupied orbital on CO is a slightly antibonding  $\sigma$  orbital ( $5\sigma$ ) mainly localized on carbon and extending beyond the internuclear vector. This may be used to  $\sigma$ -donate into an empty p or appropriately oriented  $sp^n$  hybrid on the metal, just as it donates into an empty  $d_\sigma$  orbital in a transition-metal carbonyl, to form a Lewis acid–base adduct. The lowest-lying unoccupied orbital on CO is an antibonding  $\pi$  orbital ( $2\pi$ ) mainly localized on carbon. If the main-group element possesses electrons in  $p_\pi$  orbitals, ‘back donation’ from metal to carbonyl can occur. Fig. 1 illustrates this interaction and shows

\* Non-SI unit employed: eV  $\approx 1.60 \times 10^{-19}$  J.

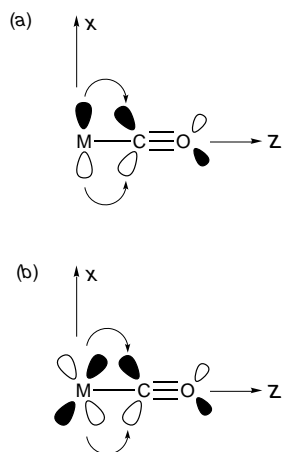
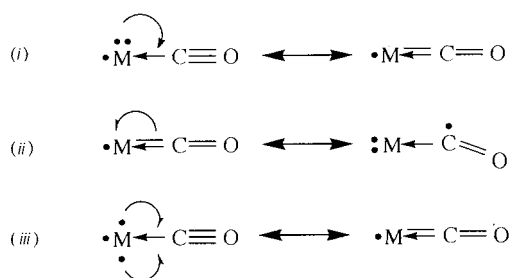
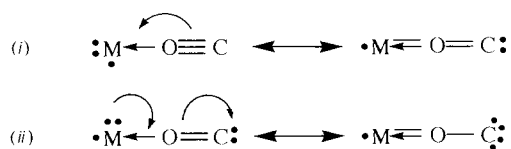


**Fig. 1** Donation of metal  $\pi_{xz}$  electron density into the  $\pi_x^*$  orbital of CO for (a) a main-group element and (b) a transition-metal element. An analogous process can take place in the  $yz$  plane



**Scheme 1**



**Scheme 2**

the analogous behaviour in transition-metal carbonyls. Scheme 1 illustrates some simple resonance forms that could be used to describe the bonding between a Group 13 metal atom and carbon monoxide.

Without structural characterization, it is possible that the complexes formed in matrices could be the isocarbonyl molecules, MOC. It is known, for example, that transition-metal carbonyl anions will co-ordinate to aluminium, gallium and indium through the oxygen atom.<sup>21</sup> The  $\pi$ -bonding orbitals ( $1\pi$ ) in free carbon monoxide are quite low in energy but are localized largely on oxygen and so a  $\pi$ -donor role for carbon monoxide into empty  $p_\pi$  orbitals on the metal might tend to favour co-ordination through oxygen. It is much more difficult to draw satisfactory resonance forms for isocarbonyl complexes. Two forms are shown in Scheme 2 showing  $\pi$  donation and  $\pi$  acceptance by the ligand. The energies and vibrational spectra for both the carbonyl and isocarbonyl complexes are reported.

Two spin states are possible for the monocarbonyl complexes. A spin doublet can be imagined to have been formed from a ground-state ( $^1\Sigma^+$ ) carbon monoxide molecule and a ground-state metal atom ( $^2P$ ) with a  $ns^2np^1$  configuration. Alternatively a spin quartet could be formed from a metal atom in an excited state ( $^4P$ ) with a  $ns^1np^2$  configuration. This configuration maximizes the possible  $\pi$ -back bonding and, as discussed more fully below, lessens the repulsion between the electrons housed in the carbon-based  $5\sigma$  orbital and those in the metal  $ns$  orbital. The energies of the lowest-lying spin-quartet and spin-doublet molecules are reported together with a discussion of the bonding in both sets of systems.

## Computational Details

Local density functional (LDF) calculations are an increasingly popular method of studying the properties of transition-metal compounds.<sup>22–25</sup> The LDF calculations reported here were performed using the DEFT code written by St-Amant<sup>26</sup> in the LCGTO framework. Two types of calculation have been completed differing in the treatment of the exchange and correlation interactions. The first, labelled 'VWN', used the Vosko–Wilk–Nusair local spin-density (LSD) approximation of the exchange-correlation potential.<sup>27</sup> The second, labelled 'BP', corrects the LSD expression using the Becke<sup>28</sup> non-local functional for exchange and the Perdew<sup>29</sup> non-local functional for correlation. These calculations follow the methods used, for example, by Fournier<sup>17,18</sup> on the analogous transition-metal monocarbonyls, Rogemond *et al.*<sup>30</sup> on  $\text{CuCl}_2$  and by Bridgeman<sup>31,32</sup> on  $\text{CuCl}_2$ ,  $\text{NiCl}_2$ ,  $\text{NiO}$  and  $[\text{NiO}_2]^{2-}$ . The results obtained on these systems were found to be at least as accurate as those achieved using sophisticated molecular-orbital-based methods. The calculations on  $\text{CuCl}_2$  and  $\text{NiCl}_2$ , for example, predicted ground states in agreement with the analysis of recent spectroscopic measurements on these systems and in contrast to those predicted by previous theoretical studies.

The Gaussian basis sets (GTOs) and the auxiliary basis sets needed for the Coulomb and exchange potential were optimized specifically for LSD calculations by Godbout *et al.*<sup>33</sup> For carbon and oxygen, GTO sets of double- $\zeta$  quality were used with the contraction patterns (721/51/41) (using Huzinaga's notation<sup>34</sup>). For boron, aluminium, gallium and indium, double- $\zeta$  basis sets with the contraction patterns (721/521/1\*), (6321/521/1\*), (63321/5321/1\*) and (633321/53321/1\*) respectively were used. All calculations were performed in an all-electron treatment. Geometry optimizations were performed for the MCO and MOC isomers starting from both linear and bent geometries and with guessed M–C and M–O bond lengths. Vibrational frequencies were calculated by finite differentiation of analytic first derivatives. Calculations were performed for the lowest-energy spin quartet and doublet for each MCO system and for the ground state of the MOC isomer. Bond energies were calculated by comparison of the energy of the MCO or MOC molecule with the total energy of the (metal atom and CO molecule) dissociation products in their ground states [ $M^2P$  ( $ns^2np^1$ ) and  $\text{CO } ^1\Sigma^+$ ] and in addition for the spin quartets with the total energy of the actual dissociation products [ $M^4P$  ( $ns^1np^2$ ) and  $\text{CO } ^1\Sigma^+$ ]. The M–C, M–O and C–O bond orders were calculated according to the prescription suggested by Mayer.<sup>35,36</sup> The calculations by Fournier<sup>17,18</sup> used one level of theory to assist comparison of the bonding in the transition-metal monocarbonyls. The calculations presented here use this same level of theory and analogous basis sets so that the bonding in the two sets of monocarbonyls may be compared.

As well as the change in CO bond length and order and the reduction in the CO stretching frequency upon complexation, the changes in Mulliken populations on CO were used to quantify the metal–carbonyl interaction. The major problem in the use of Mulliken populations to gauge charge transfer is the strong dependence of the results on the basis sets used. In the present study this problem has been reduced by the use of equivalent basis sets for each of the metal atoms. The relative degree of charge transfer along this series of closely related systems rather than the absolute values is sought. The  $\sigma$  donation, denoted  $\Delta\sigma$ , is taken to be the sum of the carbon and oxygen  $\sigma$ -orbital populations (*i.e.*  $s$ ,  $p_\sigma$  and  $d_\sigma$ ) minus six (the  $\sigma$ -orbital populations in free CO). Similarly, the  $\pi$ -back donation,  $\Delta\pi$ , is taken as the sum of the carbon and oxygen  $\pi$ -orbital populations (*i.e.*  $p_\pi$  and  $d_\pi$ ) minus four. Following the procedure used by Fournier,<sup>17,18</sup> for bent complexes the  $z$  axis is taken to lie along the CO vector, and the carbon and oxygen  $\sigma$  orbitals are defined as  $s$ ,  $p_z$  and  $d_z$  and the  $\pi$  orbitals as  $p_x$ ,  $p_y$ ,

**Table 1** Calculated equilibrium geometries for the MCO and MOC molecules

Molecule	2 <i>S</i> + 1	<i>R</i> <sub>e</sub> (M–L) <sup>a</sup> / Å		<i>R</i> <sub>e</sub> (C–O)/ Å		Bond angle/°	
		VWM	BP	VWN	BP	VWN	BP
BCO	2	1.523	1.520	1.174	1.181	160	165
	2 <sup>b</sup>	1.528	1.520	1.172	1.179	180	180
	4	1.426	1.433	1.179	1.189	180	180
BOC	4	1.393	1.406	1.250	1.270	180	180
AlCO	2	2.088	2.132	1.169	1.176	170	173
	2 <sup>b</sup>	2.099	2.136	1.168	1.176	180	180
	4	1.847	1.865	1.181	1.189	180	180
AlOC	2	1.929	1.969	1.208	1.218	180	180
GaCO	2	2.150	2.226	1.166	1.173	180	180
	4	1.816	1.845	1.184	1.193	180	180
	2	2.354	2.412	1.169	1.174	180	180
InCO	2	2.377	2.440	1.164	1.172	180	180
	4	2.039	2.074	1.179	1.187	180	180
	2	2.348	2.779	1.177	1.165	180	180

<sup>a</sup> L = C or O for the carbonyl or isocarbonyl systems respectively. <sup>b</sup> Constrained to be linear.

**Table 2** Calculated and observed vibrational wavenumbers (cm<sup>-1</sup>) for the MCO and MOC molecules

Molecule	2 <i>S</i> + 1	CO stretch			M–C stretch		Bend		Exptl. ref.
		VWM	BP	Exptl.	VWN	BP	VWN	BP	
BCO	2	1920	1881		731	722	190	241	3
	4	2059	1997	2091	1105	1082	457	481	
BOC	4	1326	1203		885	841	243	200	
AlCO	2	1942	1889	1875	387	326 *	127	132	7
	4	1911	1853		608	585	352	367	
AlOC	2	1551	1478		364	265	154	222	
GaCO	2	1954	1891	1898	284	221	132	165	7
	4	1905	1838		528	489	346	348	
GaOC	2	1856	1803		289	248	173	201	
InCO	2	1962	1896		266	219	141	173	
	4	1909	1841		450	409	278	310	
InOC	2	1869	1889		262	272	146	190	

\* Experimental 656 cm<sup>-1</sup>.

**Table 3** Calculated M–L bond dissociation energies and relative energies (both in kJ mol<sup>-1</sup>) for the MCO and MOC molecules

Molecule	2 <i>S</i> + 1	<i>D</i> [M–(CO)]		Relative energy	
		VMN	BP	VMN	BP
BCO	2	187	140	0	0
	2 *	183	138	4	2
	4	242/546	179/507	-55	-39
BOC	4	77/382	30/358	109	110
AlCO	2	131	93	0	0
	2 *	130	92	1	1
	4	6/335	-34/312	126	127
AlOC	2	52	19	79	73
GaCO	2	123	80	0	0
	4	-75/389	-125/389	198	205
GaOC	2	42	30	81	110
InCO	2	110	73	0	0
	4	-90/292	-134/254	200	209
InOC	2	46	24	64	48

\* For the spin-doublet species, the bond energy corresponds to dissociation into ground-state products [M <sup>2</sup>P (*ns<sup>2</sup>np<sup>1</sup>*) + CO <sup>1</sup>Σ<sup>+</sup>]. For the spin-quartet species, the first figure is for dissociation into ground-state products and the second for the actual dissociation products [M <sup>4</sup>P (*ns<sup>1</sup>np<sup>3</sup>*) + CO <sup>1</sup>Σ<sup>+</sup>].

*d*<sub>xz</sub> and *d*<sub>yz</sub>. Scrambling between these sets in the lower symmetry of the bent systems is ignored.

## Results and Discussion

Tables 1 and 2 list the calculated equilibrium geometries and vibrational frequencies respectively using the VWN and BP

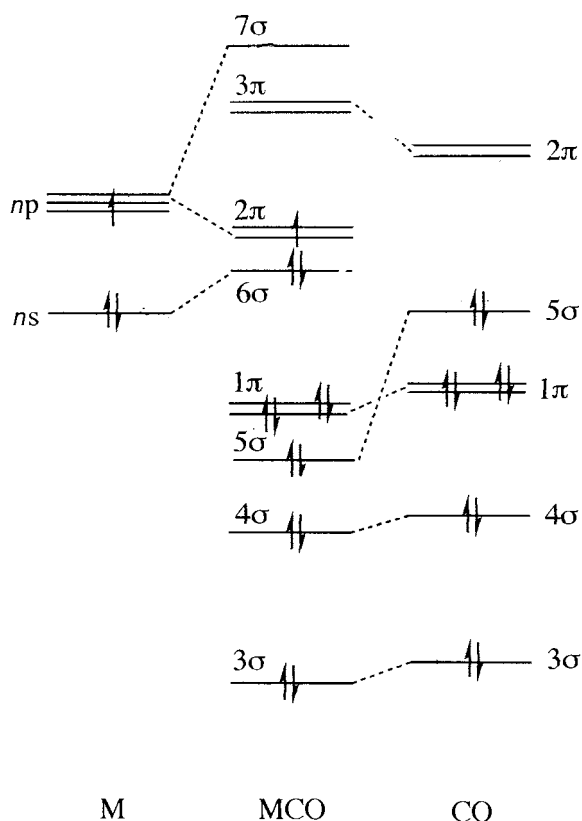
**Table 4** Mulliken populations of the Group 13 metal in the MCO molecules

Molecule	2 <i>S</i> + 1	Mulliken population			
		s	p	σ	π
BCO	2	1.6	1.5	2.4	0.8
	4	1.2	2.0	4.0	1.2
AlCO	2	1.9	0.9	2.4	0.5
	4	1.2	1.7	1.6	1.2
GaCO	2	2.0	1.0	2.5	0.5
	4	1.3	1.7	1.9	1.2
InCO	2	2.0	0.9	2.4	0.5
	4	1.3	1.7	1.8	1.2

approaches described above. The latter includes the known experimental frequencies. The description of the stretching modes as 'CO stretch' and 'M–L stretch' is, of course, a considerable simplification especially for the lighter metals where there is considerable coupling between these modes. Table 3 lists the calculated dissociation energies of the metal–carbon monoxide bonds and the relative energies of the spin-doublet and spin-quartet metal carbonyls and of the lowest-lying isocarbonyl for each Group 13 element. Table 4 lists the metal Mulliken orbital populations for each of the MCO molecules. In each case the changes in the d-orbital populations were included in the σ and π summations but were found to be very small even for the heavier metals. No significant π-donor role for the full gallium and indium d orbitals was found. The 3d and 4d orbitals are essentially core-like in these elements. Table 5 lists the Mayer bond order and the changes to the CO ligand upon complexation. A qualitative orbital diagram for a linear

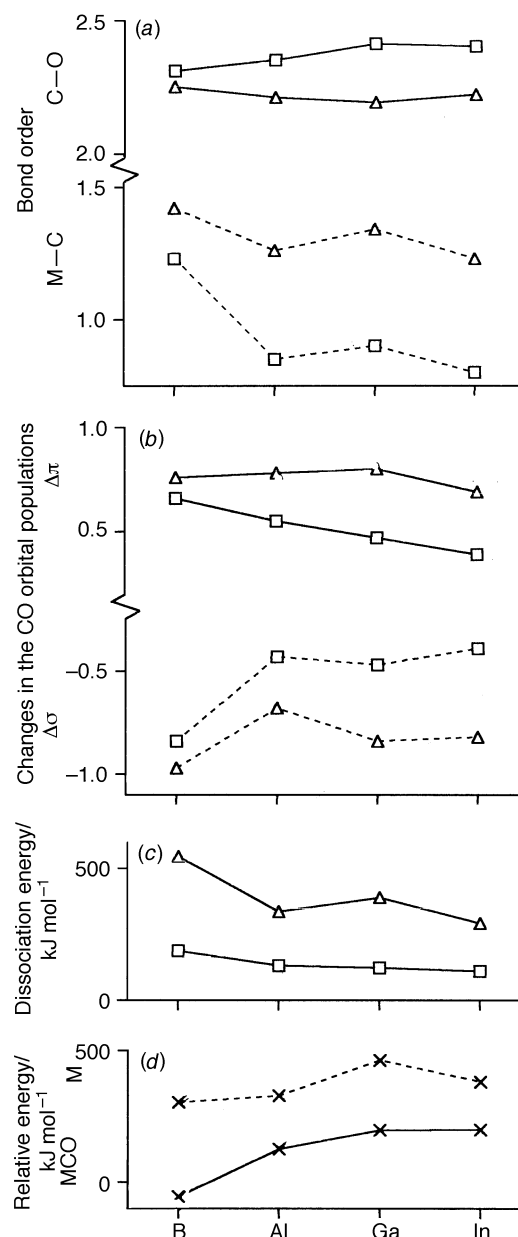
**Table 5** Bond orders for the MCO and CO molecules and the changes to CO upon complexation

Molecule	2S + 1	Bond order		Changes to CO upon complexation			
		M-C	C-O	Populations		Length $\Delta R_e/\text{\AA}$	Stretch $\Delta \omega_e/\text{cm}^{-1}$
				$\Delta\sigma$	$\Delta\pi$		
CO	1		2.54				
BCO	2	1.23	2.31	-0.84	0.66	0.05	-254
	4	1.42	2.25	-0.97	0.76	0.05	-115
AlCO	2	0.85	2.35	-0.43	0.55	0.04	-232
	4	1.26	2.21	-0.68	0.78	0.05	-263
GaCO	2	0.90	2.41	-0.47	0.47	0.04	-220
	4	1.34	2.19	-0.84	0.80	0.06	-269
InCO	2	0.80	2.40	-0.39	0.39	0.04	-212
	4	1.23	2.22	-0.82	0.69	0.05	-265

**Fig. 2** Qualitative orbital diagram for a linear main-group metal monocarbonyl

MCO molecule is illustrated in Fig. 2 and shows the orbital designations used below. Fig. 3 illustrates various calculated properties of the monocarbonyls of Group 13: (a) shows how the calculated Mayer M-C and C-O bond orders vary, (b) how the  $\sigma$  donation and  $\pi$ -back donations changes, (c) the variation in the M-C dissociation energy and (d) the relative energies of the lowest-lying spin doublet and spin quartet for both the metals and for the monocarbonyls.

The calculations predict that the ground state of BCO is  $^4\Sigma^+$  with a linear geometry. This is calculated to be  $\approx 50 \text{ kJ mol}^{-1}$  more stable than the spin-doublet form and  $\approx 110 \text{ kJ mol}^{-1}$  more stable than the isocarbonyl isomer. This ground state is consistent with the electron spin resonance spectrum<sup>3</sup> and with previous theoretical studies.<sup>3,4,37</sup> This state arises from the configuration  $(3\sigma)^2(4\sigma)^2(5\sigma)^2(1\pi)^4(6\sigma)^1(2\pi)^2$  with the three unpaired electrons housed in orbitals of primarily boron character. The calculated CO stretching frequency is in reasonable agreement with the value assigned to it in the matrix spectrum.<sup>3</sup> The lowest-lying spin-doublet state is found to be slightly bent with an angle of  $\approx 20^\circ$ . This results from bending of the lowest-

**Fig. 3** Calculated properties of the lowest-lying spin-doublet ( $\Delta$ ) and spin-quartet ( $\square$ ) states of the monocarbonyls of Group 13: (a) Mayer bond order; (b) changes in the CO orbital populations upon complexation; (c) dissociation energies, corresponding to the actual process; (d) the relative energies of the lowest-lying spin-doublet and spin-quartet states of the metal and of the MCO systems

lying linear ( $^2\Pi$ ) spin-doublet state. The  $^2\Pi$  state arises from the configuration  $\cdots (6\sigma)^2(2\pi)^1$ . Calculation of the vibrational

frequencies for the  ${}^2\Pi$  molecule results in two imaginary bending frequencies indicating that the equilibrium geometry is not linear. The energy difference between the linear and bent forms is quite small,  $\approx 2\text{--}4\text{ kJ mol}^{-1}$ , and the potential-energy curve for the molecule for the bending coordinate is rather flat for small distortions. The previous theoretical studies<sup>3,4</sup> on this system reported a linear geometry for this state although it is not clear whether linearity was calculated or assumed. This matter is discussed more fully below.

The ground state AlCO is predicted to be a slightly bent spin doublet. The bending angle is found to be  $\approx 10^\circ$ , somewhat less than that found for BCO. This state again arises from distortion of a  ${}^2\Pi$  state. The difference in energy between the linear and bent forms is small but the calculated vibrational frequencies for the linear form again suggest that it is not the equilibrium form. Previous calculations<sup>4,6,38</sup> again reported a linear geometry for this system. The ground states of GaCO and InCO are found to be  ${}^2\Pi$  and linear. For AlCO and GaCO, the CO stretching frequency calculated using the BP method particularly is in excellent agreement with the experimental value. The experimental frequency assigned to the Al–C stretch is in much poorer agreement with the calculated value for the spin-doublet ground state. No experimental studies of InCO have been reported. The lowest-lying spin quartet in each case is the  ${}^4\Sigma^+$  state with the same electronic configuration as that of the ground state of BCO.

The isocarbonyl isomers are found to be considerably less stable for each metal. For boron and aluminium isocarbonyl the CO stretching frequency is greatly reduced from its value in the free molecule and is much smaller than the experimental values. The resonance forms drawn in Scheme 2 for an MOC complex both suggest considerable weakening of the carbon monoxide bond consistent with these values. For gallium and indium the CO stretching frequencies are not sufficiently different in the MCO and MOC isomers. However, the calculated relative energies are probably large enough for the prediction to be made that the carbonyl isomers are the likely products for all four metals. The CO ligand is found to be a net  $\pi$  acceptor even when bonded to the metal through the oxygen atom. The occupied  $\pi$  orbitals on the CO ( $1\pi$ ) orbital are clearly too low in energy to interact significantly with the metal. Metal orbital overlap with the CO orbitals involved in  $\sigma$  donation ( $5\sigma$ ) and  $\pi$  acceptance ( $2\pi$ ) both strongly favour co-ordination to the carbon.

Fourniers' studies<sup>17,18</sup> on transition-metal monocarbonyls predicted bent geometries for the high-spin state MCO complexes with  $M = \text{V--Cu}$ . When the transition metal is in a  $d^{n-1}s^1$  configuration there is a two-orbital, three-electron repulsive interaction between the metal  $4s$  electron and the  $5\sigma$  donor pair on CO. Bauschlicher *et al.*<sup>39</sup> have attempted to quantify this repulsive interaction. Hybridization between the  $4s$  and an empty  $3d$  orbital acts to decrease this repulsion and strengthen the M–C bond. Where the  $sd$  hybridization is small (or if there are no empty metal  $d$  orbitals), a bent geometry results because of the repulsion between the  $4s$  electron and the  $5\sigma$  donor pair. Fournier, for example, reports that the semioccupied copper  $4s$  orbital is destabilized by  $\approx 1.4\text{ eV}$  in linear CuCO but only by  $\approx 0.8\text{ eV}$  in the bent form.

The bending of the  ${}^2\Pi$  state of BCO and AlCO appears to have a similar origin. When the metal is in the  ${}^2P$  ( $n s^2 n p^1$ ) ground state there is repulsive interaction between the metal  $n s^2$  electrons and the  $5\sigma$  donor pair on CO. Bending the molecule results in a considerable stabilization of the metal  $n s^2$  electrons housed in the  $6\sigma$  orbital and, especially in the case of boron, a significant stabilization of the core  $(n-1)s^2$  electrons. In BCO, for example, the energy of the  $6\sigma$  orbital decreases by  $\approx 0.4\text{ eV}$  and the boron  $1s$  orbital decreases by  $\approx 0.15\text{ eV}$  when the molecule is bent by  $20^\circ$  from linearity. The  $\pi$  bonding is not greatly affected by small distortions as it can still occur in the plane perpendicular to the bent molecule. The  $n s\text{--}5\sigma$  repulsion is much less when the metal is excited to the  ${}^4P$  ( $n s^1 n p^2$ ) state. In

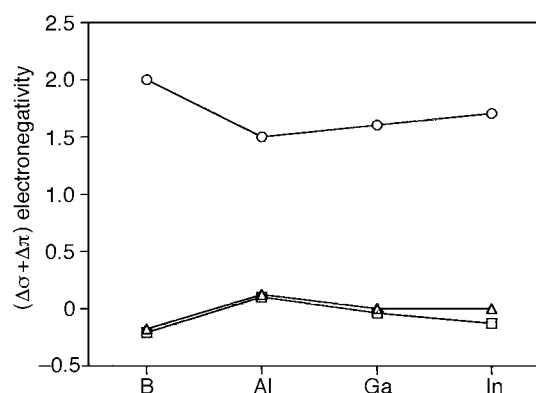


**Fig. 4** Correlation between the electronegativity of the Group 13 elements and their net  $\sigma$ -acid/ $\pi$ -base behaviour (defined as  $\Delta\sigma + \Delta\pi$ ) in the lowest-lying spin-doublet ( $\Delta$ ) and spin-quartet ( $\square$ ) states of their monocarbonyls

this state the  $\pi$ -back bonding is much reduced by bending as one metal  $p$  electron becomes effectively localized on the metal.

The repulsive role of the metal  $n s^2$  electrons is also evident in the shorter M–C bond lengths and higher M–C bond orders in the  ${}^4\Sigma^+$  state, as shown in Fig. 3(a). In exciting the metal from a  ${}^2P$  to a  ${}^4P$  state a repulsive  $n s$  electron is promoted into a  $p$  orbital where it can be used to  $\pi$ -back bond to the ligand. In the  ${}^4\Sigma^+$  state greater carbonyl-to-metal  $\sigma$  donation and metal-to-carbonyl  $\pi$ -back donation are possible. The Mulliken populations in Table 4 and the values for  $\Delta\sigma$  and  $\Delta\pi$  listed in Table 5 and shown graphically in Fig. 3(b) reflect these observations completely. The result is that the M–C bond orders are higher and the C–O bond orders lower in the  ${}^4\Sigma^+$  state, as shown in Table 5.

The dissociation energies are shown in Table 3. For GaCO and InCO and for AlCO in the BP calculations the  ${}^4\Sigma^+$  state is found to be unstable with respect to dissociation into the ground-state metal and carbon monoxide. This is due to the large promotion energy required in these metals to obtain the  ${}^4P$  state. When this promotion energy is removed by calculating the bond energy for dissociation into the metal in the  ${}^4P$  state the dissociation energies are all greater than for the spin-doublet systems as predicted by the bond orders discussed above. Fig. 3(c) shows how these bond energies and those for the spin-doublet systems vary down the Group. Fig. 3(d) shows a comparison of how the relative energies of the spin-doublet and -quartet MCO molecules and of the  ${}^4P$  and  ${}^2P$  states of the metals vary down the Group. The apparent instability of the carbonyls in the  ${}^4\Sigma^+$  state for the heavier elements is primarily due to the increasingly large  ${}^4P\text{--}{}^2P$  energy separation. The dissociation energies for the monocarbonyls in the  ${}^4\Sigma^+$  state are all fairly large and suggest that these molecules could be quasi-stable.

The M–C bond orders and dissociation energies, shown in Fig. 3(a) and 3(c), in both spin states tend to decrease down the Group. This reflects the tendency for the magnitudes of the  $\sigma$  donation ( $\Delta\sigma$ ) and the  $\pi$ -back donation ( $\Delta\pi$ ) to decrease down the Group, presumably because of the increasing M–C bond lengths and decreasing orbital-energy match and overlap. The electronegativity of these elements decreases<sup>40</sup> from boron to aluminium but *increases* from aluminium to indium. This is reflected in the  $\sigma$ -acid and  $\pi$ -base behaviour of these atoms in their monocarbonyls. Fig. 4 shows how the net acceptor/donor character of the metal atom in the monocarbonyl (defined as  $\Delta\sigma + \Delta\pi$ ) and the electronegativity of the metal vary down the Group. The correlation between the two properties is marked. Boron is a net acceptor reflecting its high electronegativity. Gallium and indium essentially achieve electroneutrality as  $\Delta\sigma$  and  $\Delta\pi$  are approximately equal in magnitude. Aluminium alone acts as a net donor reflecting its low electronegativity.

The variation in the CO stretching frequency ( $\omega_c$ ) down the

Group is shown in Table 2 and is somewhat more complicated. In transition-metal carbonyl complexes the variation in  $\omega_s$  is often taken as an indication of the extent of the  $\pi$ -back donation. No such correlation is evident in the results reported here. A similar conclusion was reported by Fournier<sup>18</sup> for the transition-metal monocarbonyls. Coupling between M–C and C–O stretching modes is presumably responsible for the complicated behaviour. The increasing mass of the metal atom down the Group will tend to reduce all vibrational frequencies whereas the C–O bond order on the whole increases down the Group leading to high vibrational frequencies.

A number of the transition-metal monocarbonyls including NiCO and CuCO have been observed<sup>41–43</sup> in the gas phase. The dissociation energy of NiCO is estimated<sup>44</sup> to be  $\approx 170$  kJ mol<sup>-1</sup> whilst that of CuCO is much lower<sup>41</sup> at  $\approx 30$  kJ mol<sup>-1</sup>. These figures suggest that all of the monocarbonyls of the Group 13 elements might be observable in the gas phase. Indium carbonyl is predicted to have similar stability to GaCO and so should be stable enough to be detectable, at least in a matrix. The most stable molecule in this set appears to be the BCO molecule and this is sometimes observed<sup>3</sup> as an impurity in the electron spin resonance spectrum of boron clusters.

## Conclusion

The structures of the monocarbonyls and isocarbonyls of the Group 13 elements have been optimized using LDF calculations in the LCGTO framework. For each metal the carbonyl complex is predicted to be considerably more stable than the isocarbonyl isomer. The ground state of BCO is predicted to be a  $^4\Sigma^+$  state. This state becomes increasingly high in energy for the remaining elements because of the large promotion energy required to excite the metal atoms into a  $^4P$  state and the ground states of their monocarbonyls are predicted to be spin doublets. The results suggest that the lowest-lying spin doublets for BCO and AlCO may be bent although the energy difference between the linear and bent forms is quite small. No experimental reports of InCO have been published but this molecule should be stable enough to be detectable.

The  $\sigma$ -acid and  $\pi$ -base behaviour of the metals towards carbon monoxide as ligand can be quantified using the changes in the CO  $\sigma$ - and  $\pi$ -orbital populations. Mayer bond orders provide a measure of the metal–carbonyl interaction. These properties correlate well with the calculated vibrational frequencies and with the changes in the M–C and C–O bond lengths, both between the different spin states and between the different molecules.

The bending of the  $^2\Pi$  states of BCO and AlCO is favoured by the reduction in the repulsive interaction between the metals'  $ns^2$  valence electrons and the  $5\sigma$  donor electron pair localized on the carbon atom of CO. This repulsive interaction is also revealed by the shorter M–C bonds, higher M–C bond orders and greater ligand-to-metal  $\sigma$  donation in the  $^4\Sigma^+$  state. Promotion of the metal into a  $^4P$  state corresponding to a  $ns^1np^2$  configuration also allows greater  $\pi$ -back bonding. The calculated dissociation energies are, as a result, considerably higher in this spin state. The ground state of BCO is a spin quartet because of the stronger bonding and relatively small promotion energy required for boron. The promotion energy for the remaining elements is prohibitively high but the excited  $^4\Sigma^+$  states are much more strongly bonded than the ground state.

The competition between the s–p promotion energy required to achieve the low-spin states and the weaker bonding in the high-spin states mirrors the situation in the transition-metal analogues briefly outlined above. The  $^1\Sigma^+$  ground state of NiCO, for example, requires promotion of an s electron into a d orbital to achieve a  $3d^94s^1$  configuration and loss of exchange energy from pairing the spins of the s and d electrons. This *low-spin* configuration reduces the repulsive  $\sigma$  interaction and increases the attractive  $\pi$ -back donation. The  $^4\Sigma^+$  ground state

of BCO requires promotion of an s electron into a p orbital. Adoption of this *high-spin* configuration similarly increases the  $\sigma$  and  $\pi$  bonding. The high spin–low spin crossover of states has the same source in both the transition-metal and Group 13 monocarbonyls: the increase in the M–CO bonding. In the transition-metal monocarbonyls this causes low-spin ground states to be adopted for MnCO, FeCO, CoCO and NiCO where the promotion and exchange energy is not too prohibitive. In the Group 13 monocarbonyls it causes the high-spin ground state of BCO where the promotion energy is not too high.

The  $\sigma$ -acid and  $\pi$ -base behaviour of the metals in both spin states parallels their electronegativity. The analogy between the bonding in these main-group monocarbonyls and that in the more familiar transition-metal systems implied by the orbital overlaps drawn in Fig. 1 and by the resonance forms in Scheme 1 is probably most appropriate for aluminium, gallium and indium where the metal is a net donor or at least achieves approximate electroneutrality. The values for  $\Delta\sigma$  and  $\Delta\pi$  are reported here for the monocarbonyls of these elements are similar in magnitude to the analogous quantities reported by Fournier<sup>18</sup> for the first-row transition-metal atoms. Boron though appears to be a somewhat better  $\sigma$  acid than the less electronegative and larger elements of the rest of Group 13 and of the transition-metal series.

## Acknowledgements

The author would like to thank Dr. Alain St-Amant of the University of Ottawa for making the DEFT code publicly available.

## References

- 1 M. S. Dewar, *Bull. Soc. Chim. Fr.*, 1951, **18**, C71.
- 2 J. Chatt and L. A. Duncanson, *J. Chem. Soc.*, 1953, 2939.
- 3 Y. M. Hamrick, R. J. Vanzee, J. T. Godbout, W. Weltner, W. J. Lauderdale, J. F. Stanton and R. J. Bartlett, *J. Phys. Chem.*, 1991, **95**, 2840.
- 4 T. R. Burkholder and L. Andrews, *J. Phys. Chem.*, 1992, **96**, 10 195.
- 5 V. Balaji, K. K. Sunil and K. D. Jordan, *Chem. Phys. Lett.*, 1987, **136**, 309.
- 6 P. Pullumbi and Y. Bouteiller, *Chem. Phys. Lett.*, 1995, **234**, 107.
- 7 A. Feltrin, M. Guido and S. N. Cesaro, *Vib. Spectrosc.*, 1995, **8**, 175.
- 8 P. S. Bagus, C. J. Nelin and C. W. Bauschlicher, jun., *Phys. Rev. B*, 1983, **28**, 5423.
- 9 A. B. Rives and R. F. Fenske, *J. Chem. Phys.*, 1981, **75**, 1293.
- 10 C. W. Bauschlicher, jun. and P. S. Bagus, *J. Chem. Phys.*, 1984, **81**, 5889.
- 11 M. R. A. Blomberg, U. B. Brandemark, P. E. M. Siegbahn, K. B. Mathisen and G. Karlström, *J. Phys. Chem.*, 1985, **89**, 2171.
- 12 C. M. Rohlfing and P. J. Hay, *J. Chem. Phys.*, 1985, **83**, 4641.
- 13 C. W. Bauschlicher, jun., C. J. Nelin, P. S. Bagus and B. O. Roos, *J. Chem. Phys.*, 1986, **85**, 354.
- 14 M. R. A. Blomberg, U. B. Brandemark, J. Johansson, P. E. M. Siegbahn and J. Wennerberg, *J. Chem. Phys.*, 1988, **88**, 4324.
- 15 J. Koutecky, G. Pacchioni and P. Fantucci, *Chem. Phys.*, 1985, **99**, 87.
- 16 P. S. Bagus, K. Hermann and C. W. Bauschlicher, jun., *J. Chem. Phys.*, 1984, **80**, 4378.
- 17 R. Fournier, *J. Chem. Phys.*, 1993, **98**, 8041.
- 18 R. Fournier, *J. Chem. Phys.*, 1993, **99**, 1801.
- 19 C. Adamo and F. Lejl, *J. Chem. Phys.*, 1995, **103**, 10 605.
- 20 G. Pacchioni and N. Rösch, *Acc. Chem. Res.*, 1995, **28**, 390.
- 21 J. M. Burlich, M. E. Leonowicz, R. B. Petersen and R. E. Hughes, *Inorg. Chem.*, 1979, **18**, 1097.
- 22 *Local Density Approximations in Quantum Chemistry and Solid-State Physics*, eds. J. P. Dahl and J. Avery, Plenum, New York, 1989.
- 23 R. G. Parr and W. Yang, *Density-functional Theory of Atoms and Molecules*, Oxford University Press, Oxford, 1989.
- 24 *Density Functional Methods in Chemistry*, eds. J. K. Labanowski and J. W. Andelm, Springer, New York, 1991.
- 25 T. Ziegler, *Chem. Rev.*, 1991, **91**, 651.
- 26 A. St-Amant, DEFT, a FORTRAN program, University of Ottawa, 1994.
- 27 S. H. Vosko, L. Wilk and M. Nusair, *Can. J. Phys.*, 1980, **58**, 1200.
- 28 A. D. Becke, *Phys. Rev. A*, 1988, **38**, 3098.

- 29 J. P. Perdew, *Phys. Rev. B*, 1986, **33**, 8822.  
30 F. Rogemond, H. Chermette and D. R. Salahub, *Chem. Phys. Lett.*, 1994, **219**, 228.  
31 A. J. Bridgeman, *J. Chem. Soc., Dalton Trans.*, 1996, 2601.  
32 A. J. Bridgeman, *J. Chem. Soc., Dalton Trans.*, 1996, 4555.  
33 N. Godbout, D. R. Salahub, J. Andzelm and E. Wimmer, *Can. J. Chem.*, 1992, **70**, 1992.  
34 *Gaussian Basis Sets for Molecular Calculations*, ed. S. Huzinaga, Elsevier, New York, 1984.  
35 I. Mayer, *Chem. Phys. Lett.*, 1983, **97**, 270.  
36 I. Mayer, *Int. J. Quantum Chem.*, 1984, **26**, 151.  
37 A. Skancke and J. F. Liebman, *J. Phys. Chem.*, 1994, **98**, 13 215.  
38 S. S. Wesolowski, T. D. Crawford, J. T. Hermann and H. F. Schäfer, *J. Chem. Phys.*, 1996, **104**, 3672.  
39 C. W. Bauschlicher, jun., L. A. Barnes and S. R. Langhoff, *Chem. Phys. Lett.*, 1988, **151**, 391.  
40 N. N. Greenwood and A. Earnshaw, *Chemistry of the Elements*, Pergamon, Oxford, 1986.  
41 M. A. Blitz, S. A. Mitchell and P. A. Hatchett, *J. Phys. Chem.*, 1991, **95**, 8719.  
42 M. J. McQuaid, K. Morris and J. L. Gole, *J. Am. Chem. Soc.*, 1988, **110**, 5280.  
43 C. E. Brown, S. A. Mitchell and P. A. Hatchett, *Chem. Phys. Lett.*, 1992, **191**, 175.  
44 L. S. Sunderlin, D. Wang and R. R. Squires, *J. Am. Chem. Soc.*, 1992, **114**, 2788.

Received 18th September 1996; Paper 6/06474D